Effect of slip velocity on hydromagnetic squeeze film between rough porous circular plates

R. M. Patel[#1], G. M. Deheri[#2] and P. A. Vadher[#3]

[#] 1. Department of Mathematics, Gujarat Arts and Science College,

2 Department of Mathematics, Sardar Patel University, Vallabh Vidyanagar0

3 Department of Physics, Government Science College, Gandhinagar

#1 Gujarat University Gujarat

#2 S P university

#3 Gujarat University

rmpatel2711@gmail.com

gmdeheri@rediffmail.com

pragnavadher@rediffmail.com

Abstract— **An endeavor has been made to analyze the effect of slip velocity on the performance of a hydromagnetic squeeze film in rough porous circular plates considering the rotational inertia of the lower plate. The stochastic modeling of Christensen and Tonder has been used to account for roughness. The concerned Reynolds, type equation is solved to obtain the pressure distribution leading to the calculation of load carrying capacity. It is observed that the magnetization tries to compensate the adverse effect of roughness especially, for lower values of rotational inertia. However, for an enhanced performance the slip parameter is required to be minimized. Here, the negative skewness associated with roughness offers some assistance to the magnetization for reducing the adverse effect of porosity and rotational inertia. It is seen that a suitable choice of plate conductivities may go to some extent for improving the performance of the bearing system particularly when variance negative is involved. Lastly, it is noticed that this type of bearing system can support certain amount of load even in the absence of flow, unlike the conventional fluid based bearing systems.**

Keywords: Circular plates, porosity, roughness, slip velocity, magnetization and load carrying capacity

I INTRODUCTION

The normal approach of non-rotating parallel plates using conventional no-slip condition at the porous interface was discussed in [1 – 4]. The effect of velocity slip at the porous interface was taken into consideration for squeeze film studies in [5 – 7]. The squeeze film behavior between rotating disks for annular geometry was analyzed in [8] incorporating rotation induced inertia effects. Usual no-slip condition at the porous surface was assumed which does not comply with the actual physical situations as discussed in [9 – 10]. Squeeze film behavior between porous disks to include the effect of velocity slip at the fluid and porous material interface was considered in [11]. Further, the velocity slip effect on the squeeze film behavior between two rotating porous annular disks was investigated in [12]. In this investigation the slip model of [9] was used and concluded that the velocity slip decreased the load carrying capacity.

Owing to the large electrical conductivity of liquid metals, the possibilities of electromagnetic pressurization from the application of an external magnetic field have been explored and investigated to modify the performance of the bearing systems. This electromagnetic pressurization comes into existence when a large external electromagnetic field through the electrically conducting lubricant is employed to induce circulating currents which in turn, interacts with the magnetic field to produce a body force which pumps the fluid between the bearing surfaces. As the liquid metals are good electrical conductors it becomes possible to increase the load carrying capacity by using the electromagnetic force thereby, overcoming the drawback associated with the lubricants at high temperature and low viscosity.

The hydromagnetic lubrications of porous as well as plane metal bearings have been investigated in a good number of theoretical and experimental studies [13 – 15]. The hydromagnetic theory of squeeze films for conducting lubricants between two non-conducting non-porous surfaces in the presence of a transverse magnetic field was dealt with in [16]. The study of hydromagnetic effect on the porous squeeze films wherein, annular and rectangular plates were respectively considered in [17, 18]. The behavior of hydromagnetic squeeze films between porous annular disks with tangential velocity slip was analyzed in [19].

By now, it is well established that the roughness of the bearing surfaces significantly affects the performance of the bearing systems [20 – 29]. The magnetic fluid based squeeze film behavior between rotating porous rough circular plates with a concentric circular pocket was treated in [30]. The behavior of hydromagnetic squeeze films between two conducting rough porous circular plates was discussed in [31]. The combined effect of rotational inertia and surface roughness on the squeeze film performance in parallel circular disks was analyzed in [32]. Although, the transverse surface roughness adversely affected the bearing system the investigations carried out in [33 – 35] indicated that the negative effect of roughness could be minimized by the positive effect of magnetization at least in the case of negatively skewed roughness. Therefore, it was deemed fruitful to investigate the problem of squeeze films between electrically conducting rough porous surfaces with electrically conducting lubricant in the presence of a transverse magnetic field for circular shape of the bearing surface considering velocity slip at the porous interface and rotation of the lower plate.

ANALYSIS

The geometry and configuration of the bearing system is presented in Figure – 1.

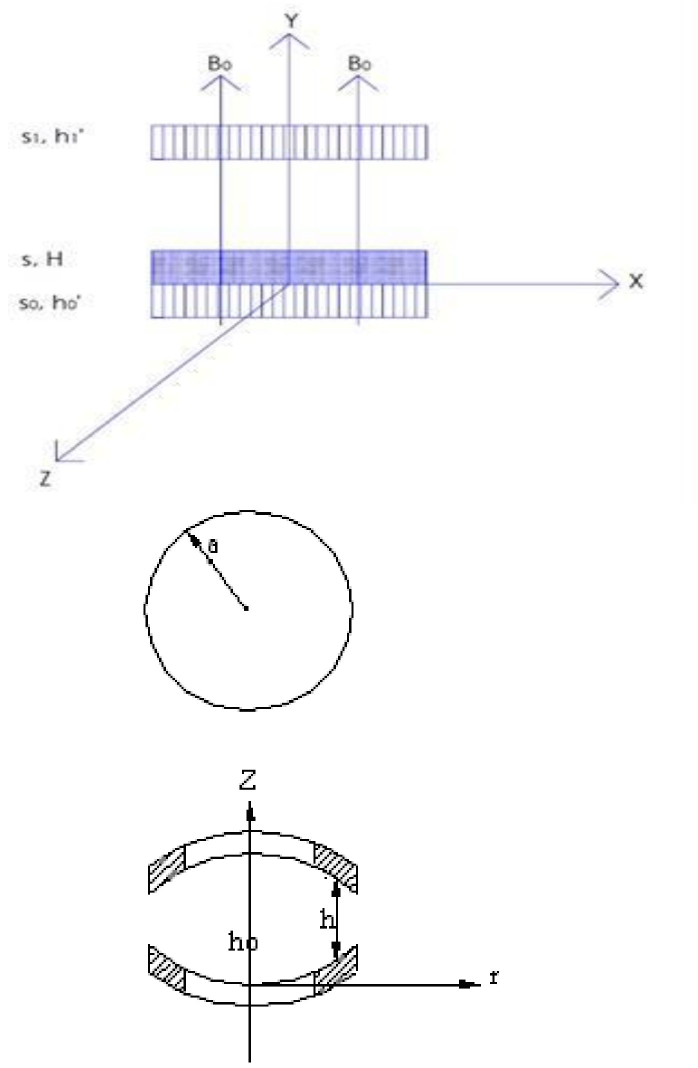

Figure – 1 Configuration of the bearing system

The lower plate with a porous facing is assumed to be rotating while the upper plate moves along its normal towards the lower plate. The plates are considered electrically conducting and the clearance space in between are filled by an electrically conducting lubricant. A uniform transverse magnetic field is applied between the plates.

When the bearing material is porous, the flow of the lubricant takes place not only in the film region but also in the porous matrix across the bearing surface – film interface. In this case, there is a coupling between the flow in the film region and that in the porous matrix. In such a situation equation governing the flow of lubricant in the porous matrix; called Darcy law is required to be solved along with Navier – Stokes equations governing the flow fields in the film region. The conventional Darcy law for velocity of the lubricant in the porous region is

$$\vec{Q} = -\frac{k}{\mu}\nabla p$$

where k is the permeability of the porous matrix and p is the lubricant pressure in the porous region.

The modified Darcy law for velocity $\vec{Q}$ of the magnetic fluid lubricant in the porous region turns out to be

$$\vec{Q} = -\frac{k}{\mu}\left(\nabla p - \vec{J}\times\vec{B}\right)$$

Following the discussions in [20 – 22] the film thickness is assumed to be of the form

$$h(x) = \bar{h}(x) + h_s(x)$$

where $\bar{h}(x)$ is the nominal film thickness between the mean level of the bearing surfaces and $h_s(x)$ is the random deviation from the mean film thickness governed by a probability density function $f(h_s)$; $-C \le h_s \le C$; where C is the maximum deviation from the mean film thickness. The mean α, the standard deviation σ and the measure of symmetry ε are defined and discussed in [37] and [20 – 22].

In view of Beavers and Joseph's slip model [9], following the method in [35], equation (E20) leads to the following:

$$\frac{1}{r}\frac{\partial}{\partial r}\left(\frac{\partial p}{\partial r}\right)=\frac{\dot{h}}{D_0 E}+G_0 \qquad (1)$$

where

$$\xi=\frac{3\eta(2\alpha_0^2\eta+h)}{h(\eta+h)},$$

$$D_0=h^3(1+\xi)\left[\frac{\psi}{\mu c^2}-\frac{2}{\mu M^3}\left\{\tanh(M/2)-(M/2)\right\}\right],$$

$$E=\left[\frac{\phi_0+\phi_1+1}{\phi_0+\phi_1+\frac{\tanh(M/2)}{(M/2)}}\right]$$

and

$$G_0=\frac{3\rho\Omega_l^2 h^3(1+\xi)}{5[h^3(1+\xi)+12kH]}.$$

As a result with usual assumptions of hydromagnetic lubrication theory and following the method of [38] and [33], one arrives at the associated stochastically averaged Reynolds' type equation resorting to the roughness model discussed in [20 – 22]:

$$\frac{1}{r}\frac{\partial}{\partial r}\left(\frac{\partial p}{\partial r}\right)=\frac{\dot{h}}{DE}+G \qquad \dots (2)$$

where

$$g(h) = h^3 + 3\sigma^2 h + 3h^2\alpha + 3h\alpha^2 + 3\sigma^2\alpha + \alpha^3 + \varepsilon,$$

$$D=g(h)(1+\xi)\left[\frac{\psi}{\mu c^2}-\frac{2}{\mu M^3}\left\{\tanh(M/2)-(M/2)\right\}\right],$$

and

$$G=\frac{3\rho\Omega_1^2 g(h)(1+\xi)}{5[g(h)(1+\xi)+12kH]}.$$

With the aid of boundary conditions

$$p(a) = 0;\ \frac{\partial p}{\partial r} = 0 \text{ at } r = 0 \qquad \dots (3)$$

solving equation (2), one obtains the pressure distribution in the form

$$p=\left(\frac{\dot{h}}{DE}+G\right)\left(\frac{r^2-a^2}{4}\right) \qquad \dots (4)$$

Using the dimensionless quantities

$$R=\frac{r}{a} \qquad \sigma^*=\frac{\sigma}{h} \qquad \alpha^*=\frac{\alpha}{h} \qquad \varepsilon^*=\frac{\varepsilon}{h^3}$$

$$S = -\frac{h^3 \rho \Omega^2}{\mu \dot{h}}$$

one derives the expression of non-dimensional pressure distribution:

$$P = -\frac{p h^3}{\mu \dot{h} a^2} = \left(\frac{1}{\bar{D}\,\bar{E}} - S\,\bar{G}\right)\frac{(1-R^2)}{4} \qquad \ldots (5)$$

where

$$g(\bar{h}) = 1 + 3\sigma^{*2} + 3\alpha^{*} + 3\alpha^{*2} + 3\sigma^{*2}\alpha^{*} + \alpha^{*3} + \varepsilon^{*},$$

$$\bar{D} = g(\bar{h})(1+\xi)\left[\frac{\psi}{c^2} - \frac{2}{M^3}\left\{\tanh(M/2) - (M/2)\right\}\right],$$

$$\bar{E} = \left[\frac{\phi_0 + \phi_1 + 1}{\phi_0 + \phi_1 + \dfrac{\tanh(M/2)}{(M/2)}}\right]$$

and

$$\bar{G} = \frac{3g(\bar{h})(1+\xi)}{5[g(\bar{h})(1+\xi) + 12\psi]}.$$

In fact, the load is the internal pressure generated between the opposite surfaces due to the dynamic action. The load carrying capacity given by

$$w = 2\pi \int_0^a p(r) \cdot r\,dr,$$

is obtained in dimensionless form as

$$W = -\frac{w h^3}{\mu \dot{h} a^4} = \frac{\pi}{8}\left(\frac{1}{\bar{D}\,\bar{E}} - S\,\bar{G}\right) \qquad \ldots (6)$$

RESULTS AND DISCUSSIONS

One can easily notice that the effect of conductivity on the pressure distribution and load carrying capacity comes through the factor

$$\left(\frac{\phi_0 + \phi_1 + \dfrac{\tanh(M/2)}{(M/2)}}{\phi_0 + \phi_1 + 1}\right)$$

It is clear that for large values of M this tends to $\dfrac{\phi_0 + \phi_1}{\phi_0 + \phi_1 + 1}$ because $\tanh(M) \to 1$, $(2/M) \to 0$. But both these functions are increasing functions of $\phi_0 + \phi_1$. It may be seen from the mathematical analysis that as $\phi_0 + \phi_1$ increases the pressure and load carrying capacity increase.

In Figures (2) – (8) one finds the variation of load carrying capacity with respect to the magnetization parameter M for various values of $\phi_0 + \phi_1$, σ^*, α^*, ε^*, S, α_0 and ψ respectively. It is easy to see that the load carrying capacity increases considerably due to magnetization. Probably, this may be due to the fact that the magnetization induces an increase in the viscosity of the lubricant. Further, the load carrying capacity gets increased due to negatively skewed roughness. Similar is the trend of load carrying capacity with respect to the negative variance. It is observed that the combined effect of standard deviation and porosity causes reduced load carrying capacity.

Figures (9) – (14) depict the variation of load carrying capacity with respect to $\phi_0 + \phi_1$. These figures suggest that the load carrying capacity increases significantly with respect to $\phi_0 + \phi_1$, the increase being more, initially. It is indicated that the variance has a very sharp impact as compared to the skewness.

From Figures (15) – (19) one concludes that the combined effect of porosity and standard deviation is quite negative. However, the situation remains a little better in the case of negatively skewed roughness particularly when variance negative occurs. The fact that variance positive decreases the load carrying capacity while load carrying capacity is increased with respect to the variance negative, is manifest in Figures (20) – (23). Identical is the trends of load carrying capacity with respect to skewness (Figures (24) – (26)), which means, the combined effect of variance negative and negatively skewed roughness may play a crucial role in mitigating the adverse effect of porosity, standard deviation and rotational inertia.

It is seen that a better option may be the lower values of rotational inertia to get an enhanced performance as can be had from Figures (27) and (28). The last Figure (29) conveys that for augmenting the performance of the bearing system the slip parameter deserves to be reduced.

A close glance at some of the figures tends to say that the combined effect of magnetization parameter and electrical permeability can go a long way in compensating the adverse effect of porosity, standard deviation and rotational inertia keeping, the slip parameter at minimum.

II. CONCLUSIONS

In any case, for an effective performance of the bearing system the slip parameter is required to be minimized. It is noticed that the negative effect of transverse roughness can be compensated up to a large extent by suitably choosing the plate conductivities and magnetization parameters at least in the case of negatively skewed roughness by keeping the slip parameter at minimum. This compensation further enhances when negative variance is involved. Therefore, it is suggested that the roughness aspects must be carefully considered while designing the bearing system, even if a suitable magnetic strength is in place.

Acknowledgements:

The authors gratefully acknowledge the critical comments and fruitful suggestions of the reviewers / editor leading to an improvement in the presentation of the paper. In fact, the suggestions of the reviewers necessitated the inclusion of appendix

References:

1 Wu, H., (1970), Squeeze film behavior for porous annular disks, Journal of Lubrication Technology, Vol. 92, p.p.593-596.
2 Wu, H., (1972a), An analysis of the squeeze film between porous rectangular plates, Journal of Lubrication Technology, Vol. 94, p.p.64-68.
3 Prakash, J. and Vij, S. K., (1973), Load capacity and time height relations for squeeze film between porous plates, Wear, Vol. 24, p.p.309-322.
4 Murti, P. R. K., (1975), Squeeze films in curved circular plates", Journal of lubrication Technology, Vol. 97(4), p.p.650-654.
5 Sparrow, E. M., Beavers, G. S. and Hwang, I. T., (1972), Effect of velocity slip on porous walled squeeze films, Journal of Lubrication Technology, Transactions of ASME, Vol. 94, p.p.260-265.
6 Wu, H., (1972b), Effect of velocity slip on the squeeze film between porous rectangular plates, Wear, Vol.20, p.p.67-71.
7 Prakash, J. and Gururajan, K., (1999), Effect of Velocity Slip in an Infinitely Long Rough Porous Journal Bearing, Tribology Transactions, Vol.42(3), p.p.661-667.
8 Wu, H., (1971), The squeeze film between rotating porous annular disks, Wear, Vol.18, p.p.461-470.
9 Beavers, G. S. and Joseph, D. D., (1967), Boundary condition at a naturally permeable wall, Journal of fluid Mechanics, Vol. 30, p.p.197-207.
10 Beavers, G. S., Sparrow, E. M. and Magnuson, R. A., (1970), Experiment on coupled parallel flow in a channel and a boundary porous medium, Journal of Basic Engineering, Transactions of ASME, Vol. 92, p.p.843-848.
11 Prakash, J. and Vij, S. K., (1974), Effect of velocity slip on porous walled squeeze films, Wear, Vol. 29, p.p.363-372.
12 Prakash, J. and Vij, S. K., (1976), Effect of velocity slip on the squeeze film between rotating porous annular disc, Wear, Vol. 38, p.p.73-85.
13 Elco, R. A. and Huges, W. F., (1962), Magnetohydrodynamic pressurization in liquid metal lubrication, Wear, Vol. 5, p.p.198-207.
14 Kuzma, D. C., (1964), Magnetohydrodynamic squeeze films, Journal of Basic Engineering, Transactions of ASME, Vol. 86, p.p.441-444.
15 Kuzma, D. C., Maki, E. R. and Donnelly, R. J., (1964), The magnetohydrodynamic squeeze films, Journal of Fluid Mechanics, Vol. 19, p.p.395-400.
16 Shukla, J. B., (1965), Hydromagnetic theory of squeeze films, Transactions of ASME, Vol. 87, p.142-147.
17 Sinha, P. C. and Gupta, J. L., (1973), Hydromagnetic squeeze films between porous rectangular plates, Journal of Lubrication Technology, Transactions of ASME, Vol. F95, p.p.394-398.
18 Sinha, P. C. and Gupta, J. L., (1974), Hydromagnetic squeeze films between porous annular disks, Journal of Mathematical and Physical Sciences, Vol. 8, p.p.413-422.
19 Patel, K. C., (1975), Hydromagnetic squeeze film with slip velocity between two porous annular disks, Journal of

Lubrication technology, Transactions of ASME, Vol. 97, p.p.644-647.
20 Christensen, H., Tonder, K., (1969a), Tribology of rough surfaces, Stochastic models of hydrodynamic lubrication, SINTEF, Section for Machine Dynamics in Tribology, Technical University of Norway, Trondheinm, Norway, Report No.10/69-18.
21 Christensen, H., Tonder, K., (1969b), Tribology of rough surfaces, parametric study and comparison of lubrication models, SINTEF, Section for Machine Dynamics in Tribology, Technical University of Norway, Trondheinm, Norway, Report No.22/69-18.
22 Christensen, H., Tonder, K., (1970) The hydrodynamic lubrication of rough bearing surfaces of finite width, ASME-ASLE Lubrication conference Cincinnati, Ohio, October 12-15, Lub-7.
23 Ting, L. L., (1975), Engagement behavior of lubricated porous annular disks Part I : Squeeze film phase, surface roughness and elastic deformation effects, Wear, Vol. 34, p.p. 159 – 182.
24 Prakash, J. and Tiwari, K., (1982), Lubrication of a porous bearing with surface corrugations, Journal of Lubrication Technology, Transactions of ASME, Vol. 104, p.p.127-134.
25 Prajapati, B. L., (1991), Behaviour of squeeze film between rotating porous circular plates: Surface roughness and elastic deformation effects, Journal of Pure and Applied Mathematical Sciences, Vol. 33(1-2), p.p.27-36.
26 Guha, S. K., (1993), Analysis of dynamic characteristics of hydrodynamic journal bearings with isotropic roughness effects, Wear, Vol. 167, p.p.173 -179.
27 Gupta, J. L. and Deheri, G. M., (1996), Effect of roughness on the behaviour of squeeze film in a spherical bearing, Tribology Transactions, Vol. 39, p.p.99-102.
28 Andharia, P. I., Gupta, J. L. and Deheri, G. M., (1999), Effect of transverse surface roughness on the behaviour of squeeze film in a spherical bearing, Journal of Applied Mechanics and Engineering, Vol. 4, p.p.19-24.
29 Andharia, P. I., Gupta, J. L. and Deheri, G. M., (1997), Effect of longitudinal surface roughness on hydrodynamic lubrication of slider bearings, Proceedings of Tenth International Conference on Surface Modification Technologies, The Institute on Materials, Singapore, p.p.872-880.
30 Patel, R. M. and Deheri, G. M. (2003), Magnetic fluid based squeeze film behavior between rotating porous circular plates with a concentric circular pocket and surface roughness effects, International Journal of Applied Mechanics and Engineering, Vol. 8(2), p.p.271-277.
31 Vadher, P. A., Vinodkumar, P. C., Deheri, G. M. and Patel, R. M., (2008), Behavior of hydromagnetic squeeze films between two conducting rough porous circular plates, Journal of Engineering Tribology, Vol. 222(4), p.p.659-679.
32 Hsu, C. H., Lu, R. F. and Lin, J. R. (2009), Combined effects of surface roughness and rotating inertia on the squeeze film characteristics of parallel circular disks, Journal of Marine Science and Technology, Vol. 7(1), p.p.60-66.
33 Shimpi, M. E. and Deheri, G. M., (2010), Surface roughness and elastic deformation effects on the behavior of the magnetic fluid based squeeze film between rotating porous circular plates with concentric circular pockets, Tribology in Industry, Vol. 32(2), p.p. 21-30.
34 Shimpi, M. E. and Deheri, G. M., (2012), Magnetic fluid based squeeze film performance in rotating curved porous circular plates: The effect of deformation and surface roughness, Tribology in Industry, Vol. 34(2), p.p. 57-67.
35 Shukla, Snehal and Deheri, G. M., (2014), Effect of slip velocity on the performance of a magnetic fluid based squeeze film in porous rough infinitely long parallel plates, Friction and Wear Research, Vol. 2(1), p.p. 6-16.
36 Prajapati, B.L. (1995), On certain theoretical studies in hydrodynamic and electromagnetohydrodynamic lubrication. Ph. D Thesis, S.P. University, Vallabh Vidyanagar, (Gujarat), India.
37 Tzeng, S.T. and Saibel, E. (1967), Surface roughness effect on slider bearing lubrication, Journal of Lubrication Technology, Transactions of ASME, Vol. 10, p.p. 334 -338.
38 Bhat, M. V., (2003), Lubrication with a magnetic fluid, Team Spirit, India, Pvt. Ltd.

Figure: 2 Variation of load carrying capacity with respect to M and $\phi_0+\phi_1$.

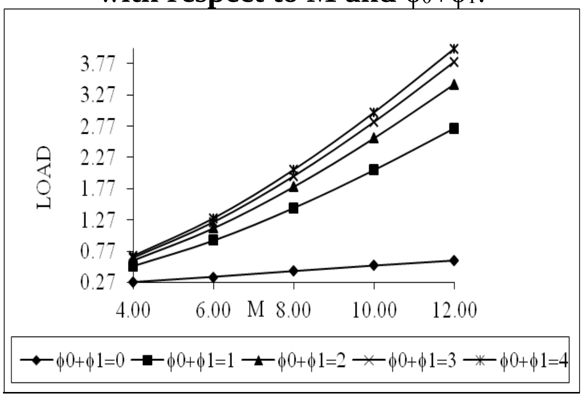

Figure: 3 Variation of load carrying capacity with respect to M and $\sigma*$.

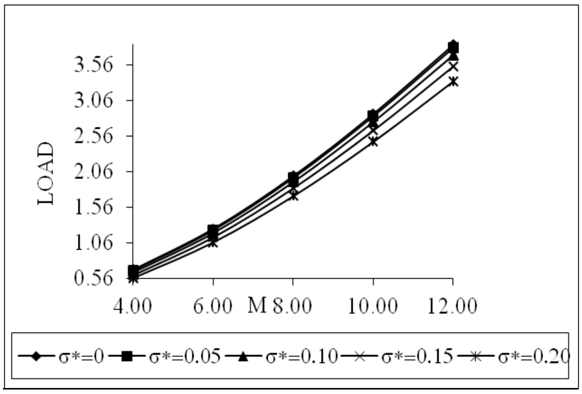

Figure: 4 Variation of load carrying capacity with respect to M and $\alpha*$.

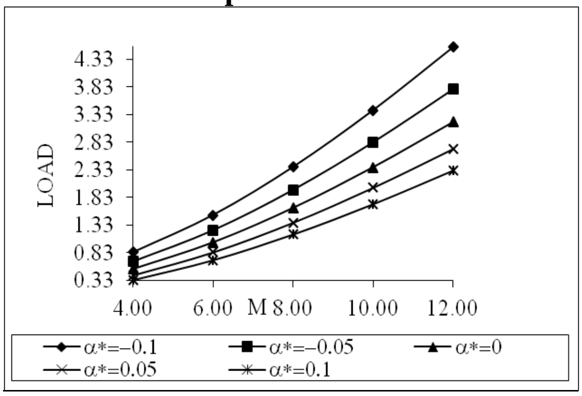

Figure: 5 Variation of load carrying capacity with respect to M and $\varepsilon*$.

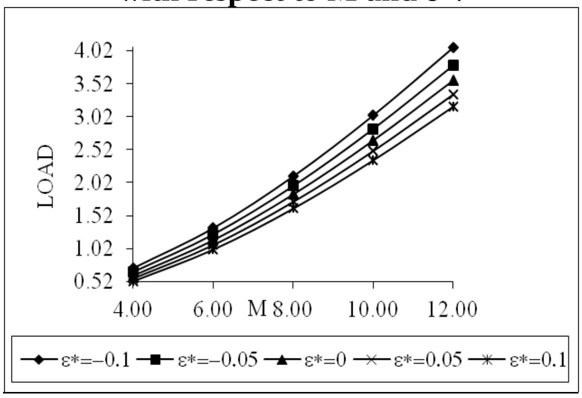

Figure: 6 Variation of load carrying capacity with respect to M and S.

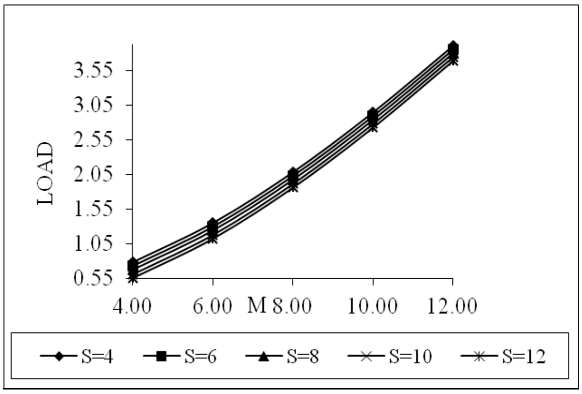

Figure: 7 Variation of load carrying capacity with respect to M and α_0.

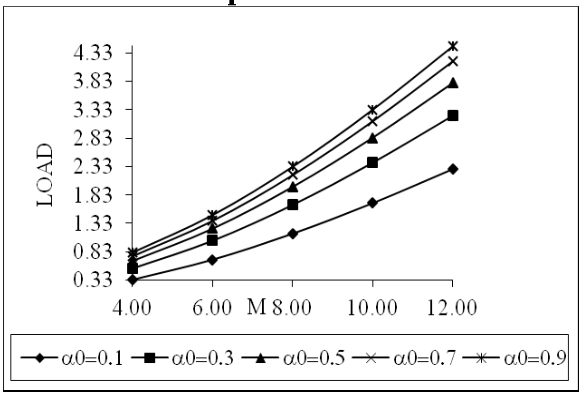

Figure: 8 Variation of load carrying capacity with respect to M and ψ.

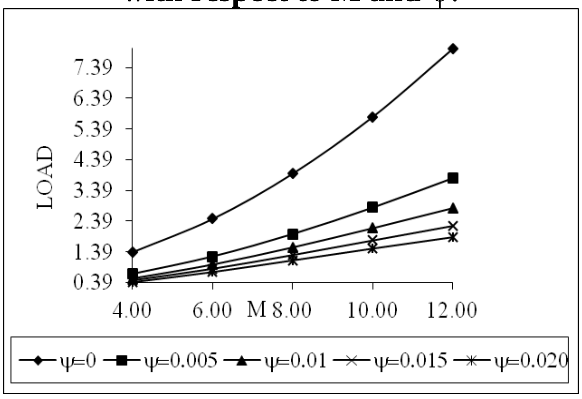

Figure: 9 Variation of load carrying capacity with respect to $\phi_0+\phi_1$ **and** $\sigma*$.

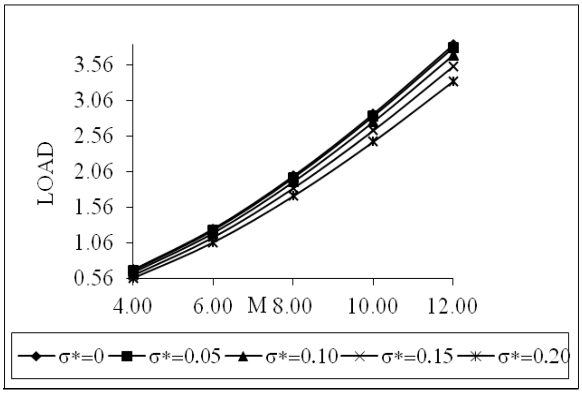

Figure: 10 Variation of load carrying capacity with respect to $\phi_0+\phi_1$ and $\alpha*$.

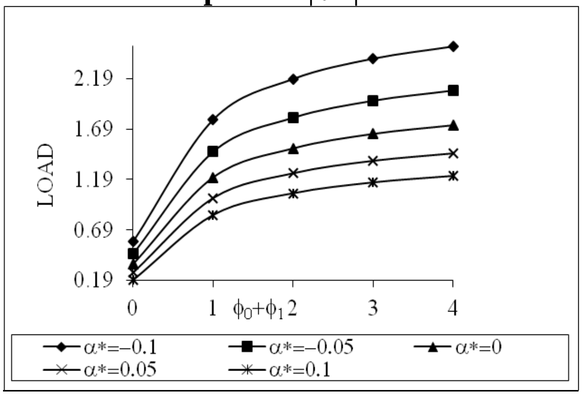

Figure: 11 Variation of load carrying capacity with respect to $\phi_0+\phi_1$ and $\varepsilon*$.

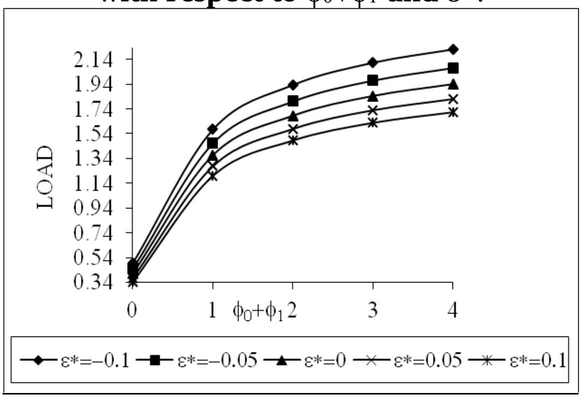

Figure: 12 Variation of load carrying capacity with respect to $\phi_0+\phi_1$ and S.

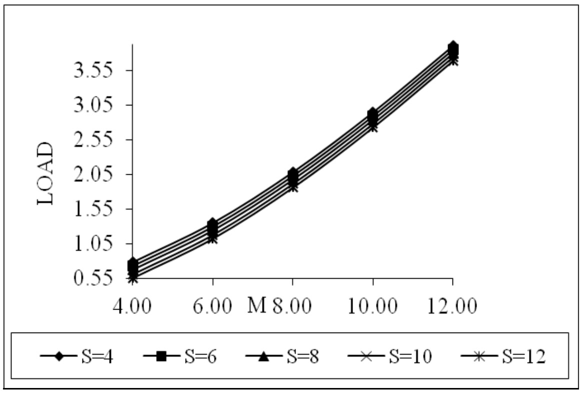

Figure: 13 Variation of load carrying capacity with respect to $\phi_0+\phi_1$ and α_0.

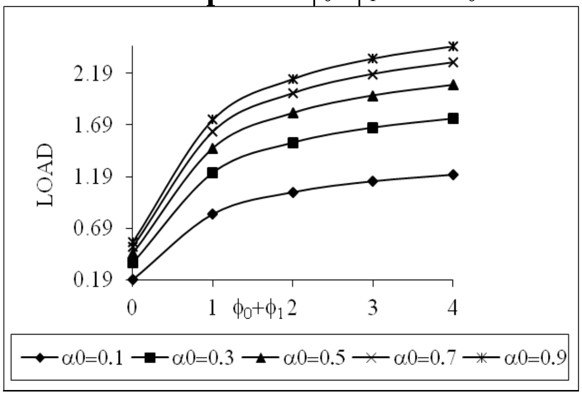

Figure: 14 Variation of load carrying capacity with respect to $\phi_0+\phi_1$ and ψ.

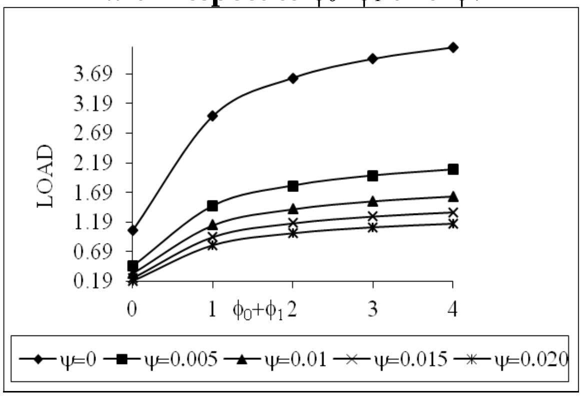

Figure: 15 Variation of load carrying capacity with respect to $\sigma*$ and $\alpha*$.

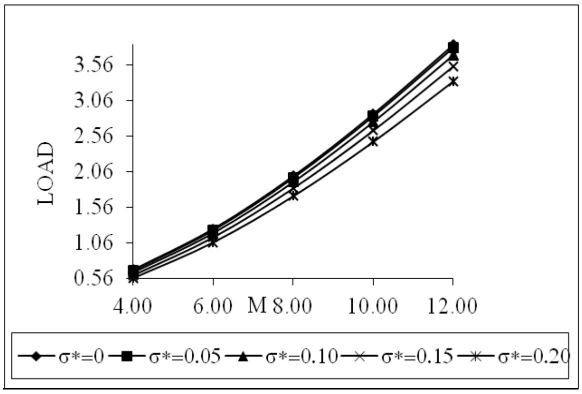

Figure: 16 Variation of load carrying capacity with respect to σ∗ and ε∗.

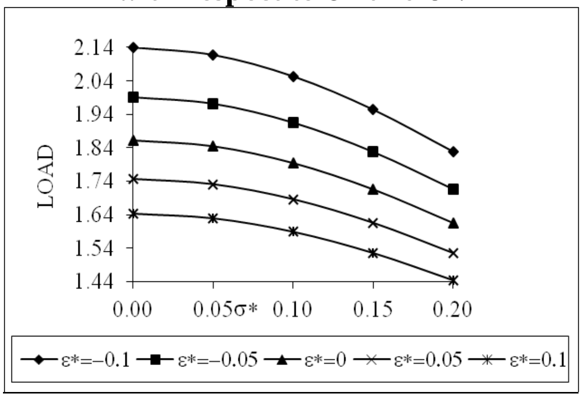

Figure: 17 Variation of load carrying capacity with respect to σ∗ and S.

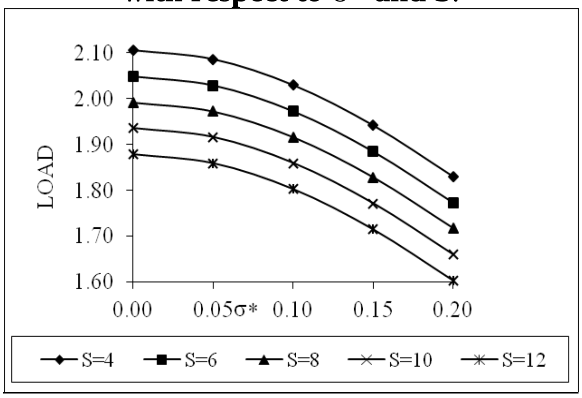

Figure: 18 Variation of load carrying capacity with respect to σ∗ and α_0.

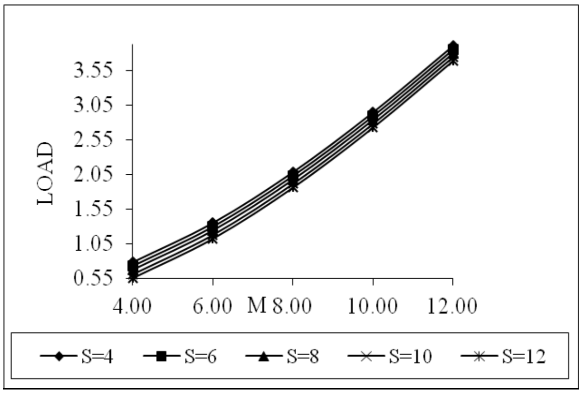

Figure: 19 Variation of load carrying capacity with respect to σ∗ and ψ.

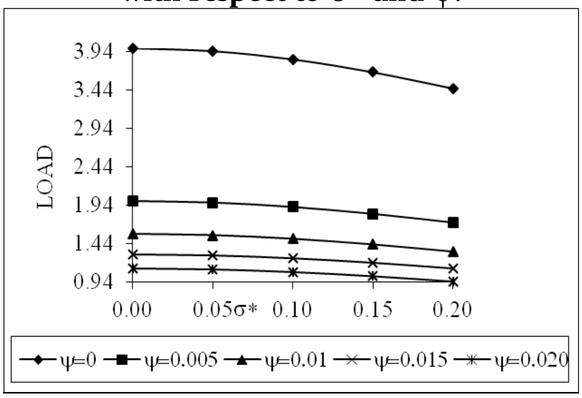

Figure: 20 Variation of load carrying capacity with respect to α∗ and ε∗.

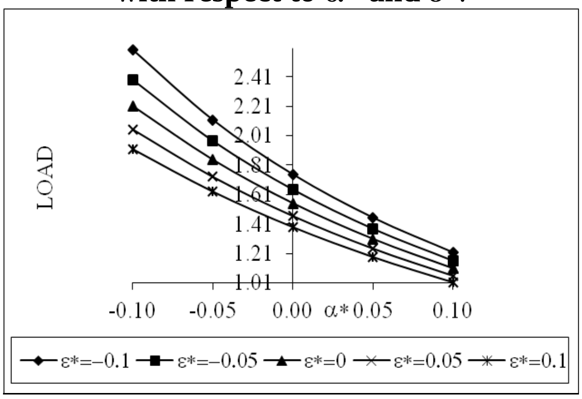

Figure: 21 Variation of load carrying capacity with respect to α∗ and S.

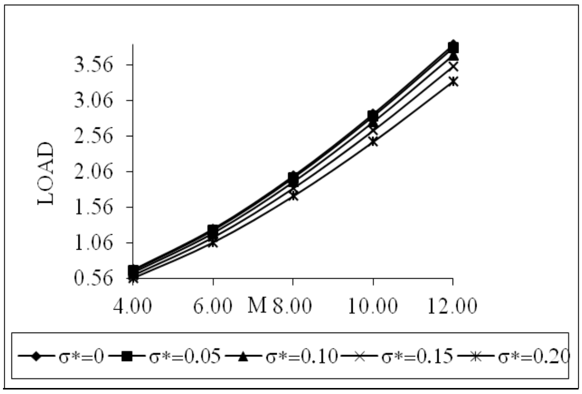

Figure: 22 Variation of load carrying capacity with respect to $\alpha*$ and α_0.

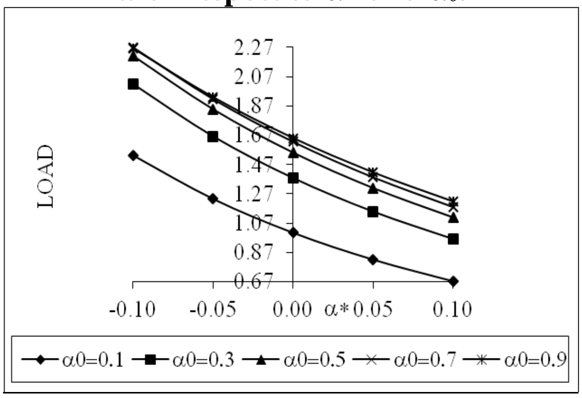

Figure: 23 Variation of load carrying capacity with respect to $\alpha*$ and ψ.

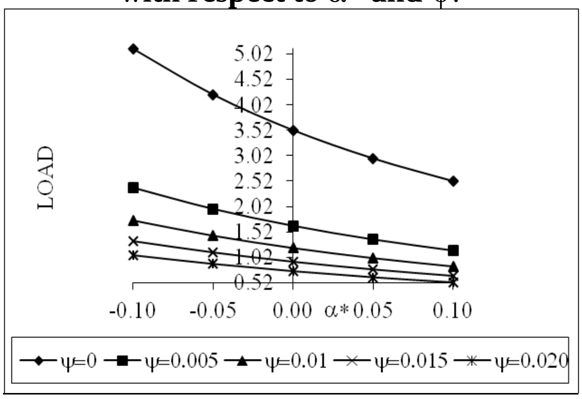

Figure: 24 Variation of load carrying capacity with respect to $\varepsilon*$ and S.

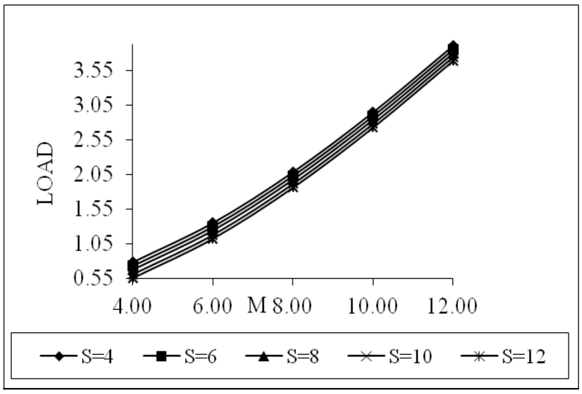

Figure: 25 Variation of load carrying capacity with respect to $\varepsilon*$ and α_0.

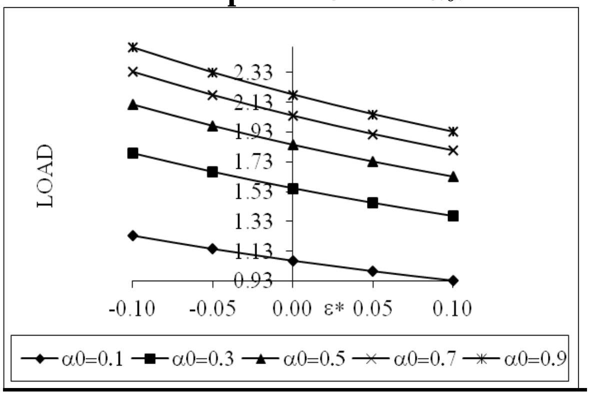

Figure: 26 Variation of load carrying capacity with respect to $\varepsilon*$ and ψ.

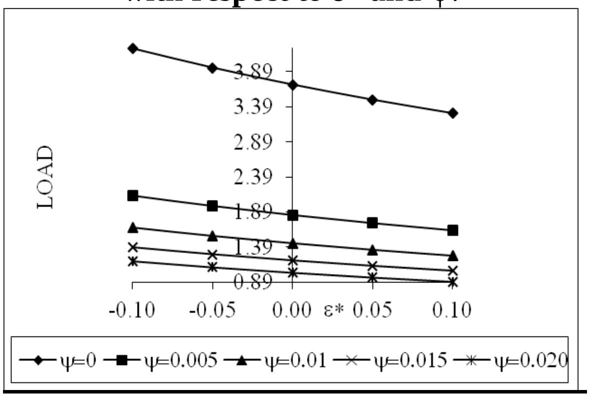

Figure: 27 Variation of load carrying capacity with respect to S and α_0.

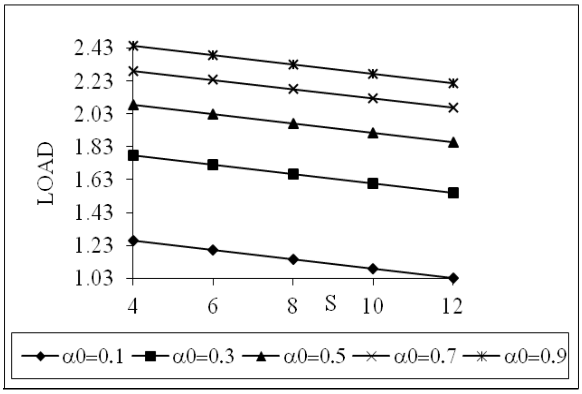

Figure: 28 Variation of load carrying capacity with respect to S and ψ.

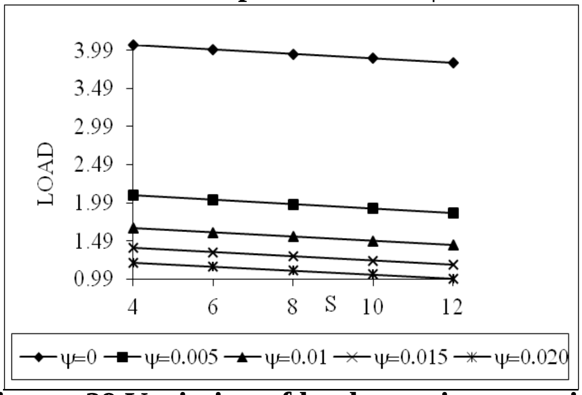

Figure: 29 Variation of load carrying capacity with respect to α0 and ψ.

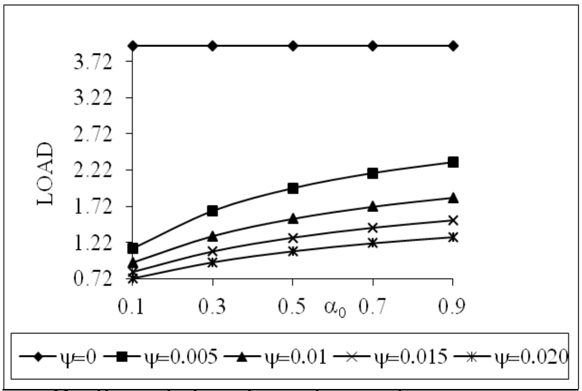

a	Radius of the plates (meter)
h	Lubricant film thickness (meter)
H	Magnetic field component
k	Permeability
m	Porosity of the porous matrix
M	$= B_0 h\left(\frac{s}{\mu}\right)^{1/2}$ = Hartmann number
p	Pressure distribution (N/m^2)
P	Non-dimensional pressure
s	Electrical conductivity of the lubricant
w	Load carrying capacity (kgm/s^2)
W	Dimensionless load carrying capacity
B_0	Uniform transverse magnetic field applied between the plates.
c^2	$= 1+\frac{KM^2}{h^2 m}$
h_0'	Surface width of the lower plate (meter)
h_1'	Surface width of the upper plate (meter)
s_0	Electrical conductivity of lower surface
s_1	Electrical conductivity of upper surface
Δt	Response time
ΔT	Non-dimensional response time
$\phi_0(h)$	$= \frac{s_0 h_0'}{sh}$ = Electrical permeability of the lower surface
$\phi_1(h)$	$= \frac{s_1 h_1'}{sh}$ = Electrical permeability of the upper surface
ψ	$= \frac{kH}{h^3}$ = Porosity
μ	Viscosity (kg/ms)
$\bar{\mu}$	Magnetic susceptibility (m^3/kg)
μ_0	Permeability of the free space (N/A^2)
σ^*	Non-dimensional standard deviation (σ/h)
α^*	Non-dimensional variance (α/h)
ε^*	Non-dimensional skewness (ε/h^3)
α_0	Slip coefficient
η	$= \frac{\sqrt{\psi}}{\alpha_0}$ = Slip parameter
ρ	Fluid density
Ω_l	Angular velocity of the lower plate
S	$= -\frac{h^3\rho\Omega_l^2}{\mu\dot{h}}$ = rotational inertia